

# Laser Metal Deposition of Ti6Al4V: A Study on the Effect of Laser Power on Microstructure and Microhardness

Rasheedat M. Mahamood, Esther T. Akinlabi, Mukul Shukla and Sisa Pityana

**Abstract—** The effect of laser power on the resulting microstructure and microhardness of laser metal deposited Ti6Al4V powder on Ti6Al4V substrate has been investigated. The tracks were deposited using 99.6 % pure Ti6Al4V powder of particle size ranging between 150 - 200  $\mu\text{m}$  on 99.6% Ti6Al4V substrate. The laser power was varied between 0.8 - 3.0 kW while the scanning speed, powder flow rate and the gas flow rate were kept at the values of 0.005 m/sec, 1.44 g/min and 4 l/min respectively. The microstructure and the microhardness were studied using the optical microscope and the Vickers hardness tester respectively. Layer band or macroscopic banding was observed in all the samples which is phenomenon as it was only reported in the literature for multi-layer deposits. The literature attributed re-melting of the previous layers by the succeeding layers as being responsible for their formation. This study has revealed that this band could be as a result of shrinkage happening in the fusion zone as a result of the interaction of the deposited powder and the melt pool created by the substrate material. This study also reveals the relationship between the microstructure, the average microhardness and the laser power which are comprehensively discussed. The higher the laser power, the lower the density of columnar prior beta grain structure. Also the average microhardness increases as the laser power increases.

**Keywords—** Laser Metal Deposition Process, Laser power, Ti6Al4V, Macroscopic Banding, Microhardness, Microstructure.

Manuscript received September 21, 2012; revised November 10, 2012. This work was supported by the Rental Pool Grant of the National Laser Centre -Council of Scientific and Industrial Research (NLC-CSIR), Pretoria, South Africa and The Schlumberger Foundation Faculty for the Future (FFTF).

Ms. Rasheedat M. Mahamood is a doctorate Student in the Department of Mechanical Engineering Science, University of Johannesburg, Auckland Park Campus, Johannesburg, South Africa, 2006. (e-mail: mahamoodmr@unilorin.edu.ng or mahamoodmr@yahoo.com)

Dr Esther T. Akinlabi is a Senior Lecturer in the Department of Mechanical Engineering Science, University of Johannesburg, Auckland Park Campus, Johannesburg, South Africa, 2006. (Phone: +2711-559-2137; email: etakinlabi@uj.ac.za).

Prof Mukul Shukla is an Associate Professor in the Department of Mechanical Engineering Science, University of Johannesburg, Auckland Park Campus, Johannesburg, South Africa, 2006. (e-mail: mshukla@uj.ac.za).

Prof Sisa Pityana is a Research Scientist in the National Laser Centre of Council for Scientific and Industrial Research (CSIR), Pretoria, South Africa. (E-mail: SPityana@csir.co.za.)

## I. INTRODUCTION

Ti6Al4V is the most commonly produced titanium alloy and also the most commonly used titanium alloy in the aerospace industry [1, 2]. This is because Ti6Al4V possesses excellent structural and corrosion resistance properties [3-5]. Titanium and its alloys are classified as generally difficult to machine material [6] because of the high interaction between the titanium and the cutting tool materials thereby causing high temperature and galling the cutting tool that shortens the tool life [6]. Also, a series of heat treatment is also required when cutting titanium and its alloys because of heat hardening that occurs during the cutting operation. With all these difficulties in machining titanium through traditional manufacturing processes, there is need for alternative manufacturing technique that will offset most of these difficulties; the candidate manufacturing method is Additive Manufacturing (AM) method. Additive manufacturing as the name implies process material through addition of material in layer wise fashion [7] unlike in traditional manufacturing, cutting operation for example, that removes material to shape a component.

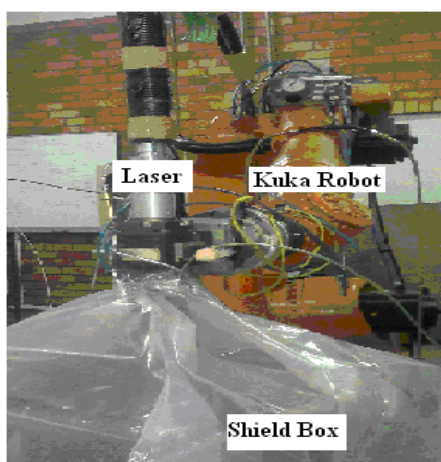
Laser Metal Deposition (LMD) is an additive manufacturing technique that produces solid components directly from CAD model file [8,9]. Of all the additive manufacturing techniques, LMD is unique in that it can be used to effect repair of high valued component parts which were discarded in the past [10]. LMD can also be used to produce functionally graded materials [11] because it can handle different materials at the same time. Laser metal deposition is particularly attractive for the production of aerospace parts because it can greatly increase fly-to-buy ratio [12,13]. Also, the repair of high valued components can readily be achieved in situ with laser metal deposition process [14,15].

The Laser metal deposition process is achieved by feeding powder, which is assisted by shielding gas, into the melt pool that is generated by sharply focused collimated laser beam on the substrate. The interaction between the substrate and the laser create the melt pool. A lot of work has been reported in the literature on laser metal deposition of titanium alloys [4,12,13], most of which investigated a combination of parameters effect on the property of the deposited Ti6Al4V. The focus of this present work is to extensively study effect of only one process parameter with the aim of easing the difficulty of developing a close loop control for full automation of laser metal deposition process. This is particularly useful in the repair process. The effect of laser power on the microstructure and the microhardness of Ti6Al4V were thoroughly investigated in this study while

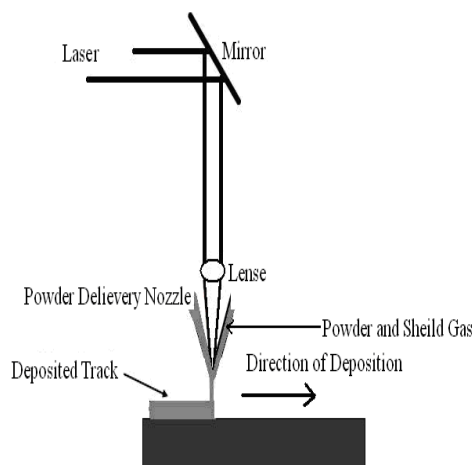
keeping the scanning speed, the powder flow rate and gas flow rate constant through out the experiments. Controlling a single variable is much more simpler in the development of a closed loop control system than using combination of variables which becomes more complex especially where interactions exists between these variables.

## II. EXPERIMENTAL TECHNIQUE

The Laser Metal Deposition (LMD) process was achieved with 4.4 kW fiber delivered Nd-YAG laser with coaxial powder nozzles. A Kuka robot was used to carry both the laser and powder nozzles and also controls the deposition process. Complete shielding of the deposit was achieved by the use of plastic material that is attached to the end effector of the robot which covers the shielding block completely during the deposition process; the photograph of the experimental setup is shown in Figure 1a. The gas assisted powder was delivered into the melt pool created by the laser on the substrate in order to generate a deposited track. The schematic of the deposition process is shown in Figure 1b.



(a)



(b)

Figure 1: (a) Experimental setup (b) Schematic of Laser Metal Deposition Process

99.6% pure Ti6Al4V substrate of dimension 72 x 72 x 5 mm thick plate was used on which the 99.6% pure Ti6Al4V powder was deposited. The particle size of the powder ranged between 150 to 200  $\mu\text{m}$ . A preliminary experiment was first conducted to establish a process window that produces fully dense, pore free and good metallurgically

bonded deposit. Based on the result of the preliminary experiment, a laser power of 800 W, scanning speed of 0.005 m/sec, powder flow rate of 1.44 g/min and a gas flow rate of 4 l/min produced a fully dense, pore free with good metallurgical bonded deposit. These parameters were used as a benchmark in this study. The scanning speed, powder flow rate and the gas flow rate were fixed at these values and only the laser power was varied between 0.8 and 3.0 kW. The process parameters are presented in Table 1.

**Table 1.** Processing parameters

Sample Designation	Laser Power (kW)	Scanning Speed (m/Sec)	Powder Flow Rate (g/min)	Gas Flow Rate (l/min)
A	0.8	0.005	1.44	4
B	1.2	0.005	1.44	4
C	1.6	0.005	1.44	4
D	2.0	0.005	1.44	4
E	2.4	0.005	1.44	4
F	2.8	0.005	1.44	4
G	3.0	0.005	1.44	4

The substrate was sand blasted and cleaned with acetone prior to the deposition process. A track length of 60 mm was deposited for each of the processing parameter set and designated as A to G in order to study the effect of the laser power changes on the evolving microstructure and the microhardness. After the deposition process, the samples were laterally sectioned and mounted in resin. The samples were ground, polished and etched according to the standard metallographic preparation of Titanium. The samples were studied under the Optical Microscopy (OM). The microhardness was performed using the Vickers hardness tester with a load of 500 g and a dwelling time of 15 seconds. The spacing between the indentations was fixed at 15 $\mu\text{m}$ .

## III. RESULTS AND DISCUSSION

The microstructure of the substrate used as observed under the optical microscope is shown in Figure 2. The macrograph of the Ti6Al4V powder used in this study is shown in Figure 3a and the particle size distribution is shown in Figure 3b. The microstructure is characterized by alpha and beta grain structure with the lighter part showing the alpha grains and the darker parts showing the beta grains. The powder is gas atomized and spherical in shape. The particle size distribution is Gaussian.

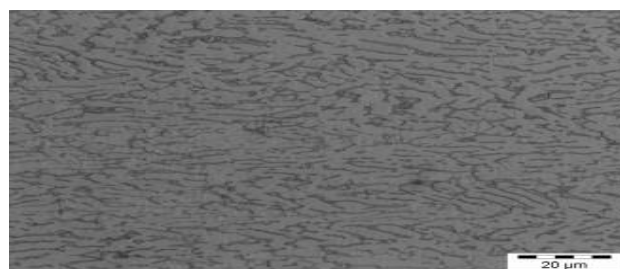
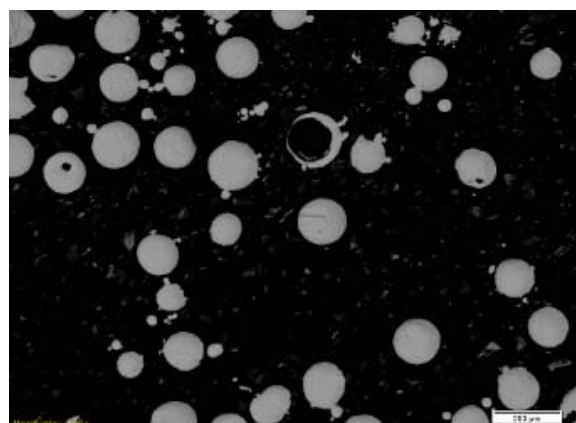


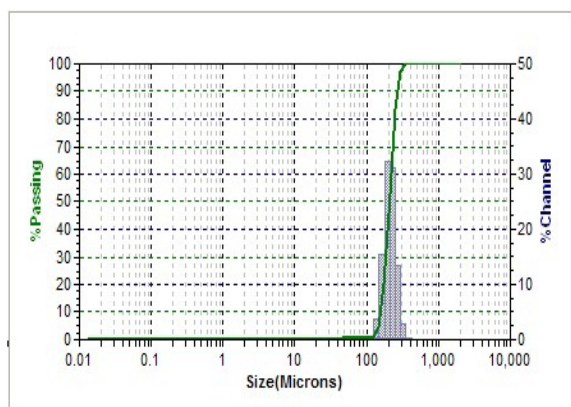
Figure 2: Microstructure of the substrate

The schematic of the deposit as viewed from the cross-section is shown in Figure 4, it is divided into three microstructure zones. The Deposit Zone (DZ) consists of the

melted deposited powder, the Fusion Zone (FZ) consists of the mixture of the substrate material and the deposited powder all melted and mixed to produce bonding of the deposited material with the substrate material. The Heat Af-



(a)



(b)

Figure 3: (a) Morphology of the Ti6Al4V powder, (b) Particle size analysis of the Ti6Al4V powder

ected Zone (HAZ) on the other hand is the substrate material that has been heated up during the deposition process. The substrate acts as a heat sink and the part of the substrate that received high enough heat to cause microstructural changes in this area is referred to as the heat affected zone. The results are divided into two parts namely: the macrostructure or morphology and microstructural results, and the microhardness results.

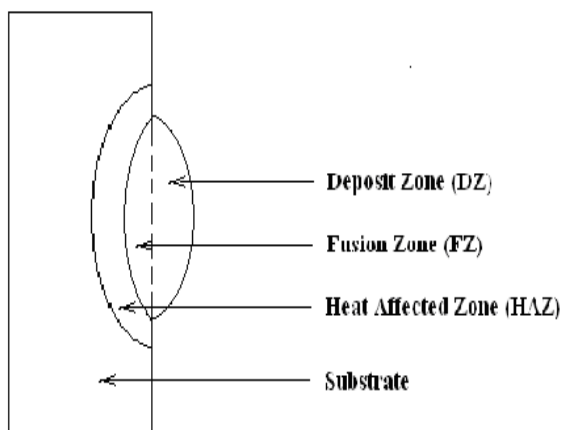


Figure 4: Schematic of the cross sectional view of the deposit on the substrate

### A Morphology and Microstructure

The morphology of the sample A is shown in Figure 5 displaying the deposit zone, the fusion zone and the heat affected zone as depicted by the Figure 4. It can be observed that the grains are continuous from the fusion zone to the deposit zone and are columnar in nature, this is seen in all the samples. Figure 6a and 6b show the sample A and sample F respectively indicating the macroscopic banding that was observed in all the samples.

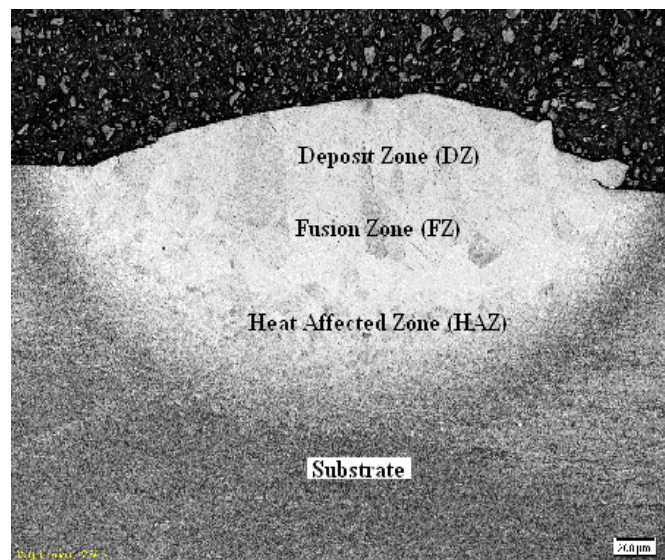
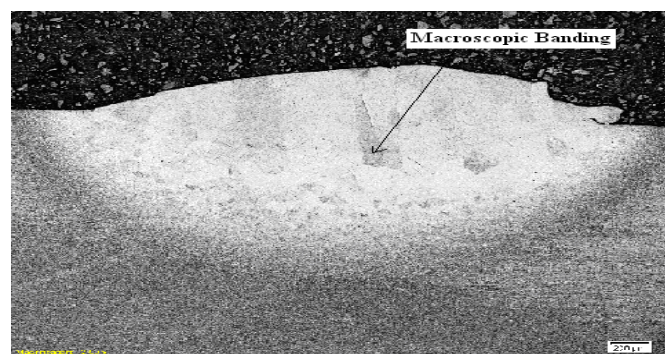
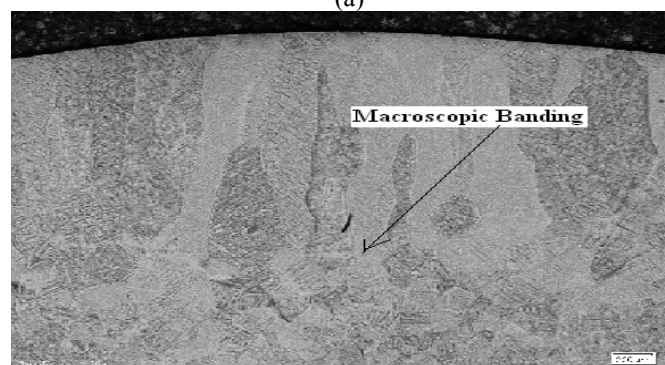


Figure 5: Morphology of Sample A showing the different zones



(a)



(b)

Figure 6: Showing Macroscopic banding of (a) sample A (b) Sample F

The macroscopic observation (see Figure 5) revealed that the deposit zone and the fusion zones were characterized by continuous columnar prior  $\beta$  grains, this is the characteristics of Ti6Al4V whether casted [12] or laser

deposited [16] but it is worthy to note that the macroscopic banding or layer band are seen in all the samples (see Figure 6) as opposed to what is seen in the literature which is common to only multi - layer deposits [16]. This banding are often attributed to reheat of the previous layer by the succeeding layer thereby creating another heat affected zone [16]. Only single layer was deposited for each of the processing parameter in this study and yet these bands were observed. It can be inferred that these banding were not as a result of reheating of the layer and it could be attributed to the interaction in the fusion zone. The fusion zone must have experienced some kind of shrinkage during solidification as a result of mixing action taking place. Figure 7 shows the microstructure of sample G indicating the various alpha grains and the microstructure at the band area. As can be seen, the change in the microstructure of the band area is localised (see Figure 7) to a particular grain which further explains that this could be due to shrinkage in this location as a result if gas escape during solidification of the fusion zone as all the bands are seen in the fusion zone area. This require further study to understand the underlying physics of this phenomenon.

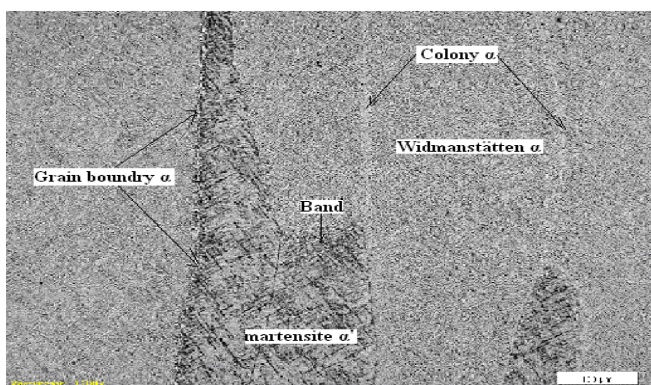
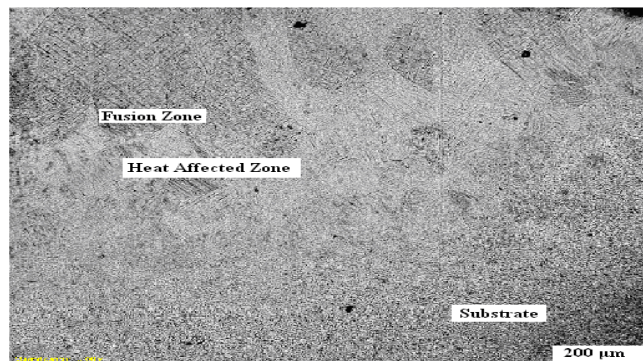


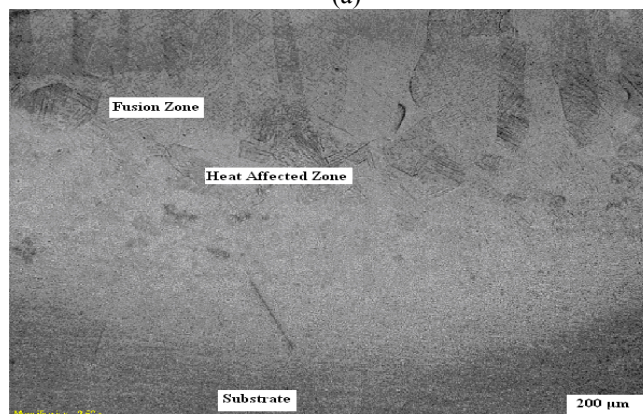
Figure 7: Microstructure of the fusion zone of Sample G showing different  $\alpha$  grains

The macrographs of the fusion and the heat affected zone of the samples B and D are presented in Figure 8. The grain growth in the deposit zones in all the samples are dominated by heterogenous nucleation; this is because the substrate material is the same as the powder material [17] and they grow epitaxially on the globular grains in the HAZ [18] (see Figure 8). The crytals at the fusion zone builds on the globular grains of the heat affected zone (see Figure 8) as observed in all the samples and the population of the globular grains in the heat affected zone decreases with increase in the laser power (see Figure 6 and 8) this is because the cooling rate decreases as the laser power increases, which results in less nucleation sites and also the melt pool stays longer on the substrate before it completely solidifies.

The longer time spent by the melt pool results in more grain growth in the heat affected zone, i.e more grains were merging together. This also translate to the fewer number of culumnar grains in the deposit zone as the laser power increases because the columnar grains grow epitaxially on the globular grains in the HAZ of the substrate.



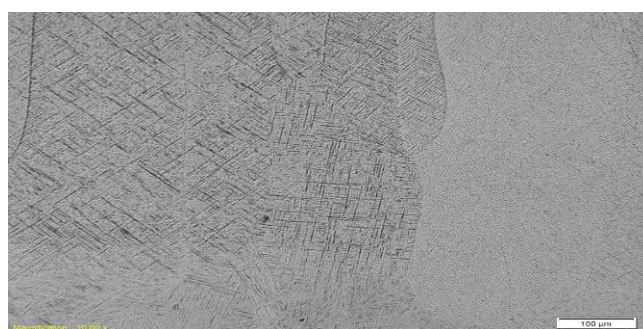
(a)



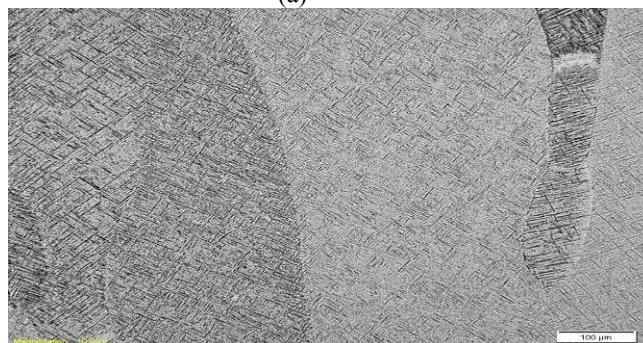
(b)

Figure 8: Macrographs showing the fusion zone and the heat affected zone of (a) sample B (c) sample D

The direction of the grain growth is opposite the maximum temperature gradient. The maximum temperature gradient is towards the substrate (heat sink), hence the grain growth direction is opposite this direction. The microstructure of the deposit zone of samples C and D are shown if Figure 9a and 9b respectively.



(a)



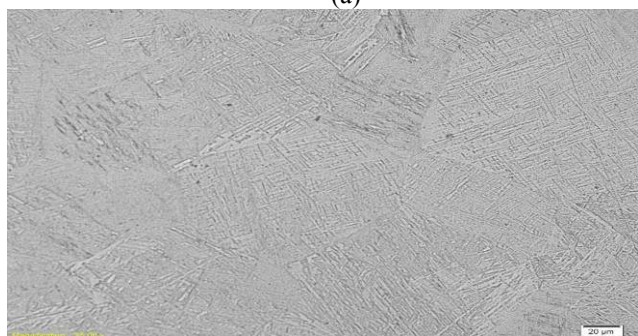
(b)

Figure 9: Microstructure of the deposit zone of (a) Sample C (b) Sample D

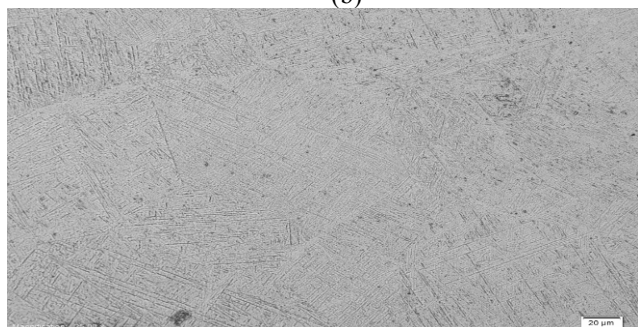
The microstructures of the heat affected zones of the samples A, C and G are shown in Figure 10. The microstructure of the heat affected zone is characterised by acicular alpha grain structure.



(a)



(b)



(c)

Figure 10: The microstructure of the heat affected zone of (a) sample A (b) sample C (c) sample G (upper part showing part of the fusion zone)

### B Microhardness

Figure 11 shows the average microhardness values of all the samples that was plotted against the samples to see the relationship between the change in average microhardness and the change in laser power. The average hardness value of each of the sample was determined and the average of the samples are plotted against the sample designation. The best fit line was drawn across the points to see the trend as shown in Figure 11. The substrate material has the lowest average microhardness value. It was observed that the average Vickers hardness value increases with increase in the laser power. This is expected because of the microstructure changes from fine microstructure to coarse microstructure as the laser power increases.

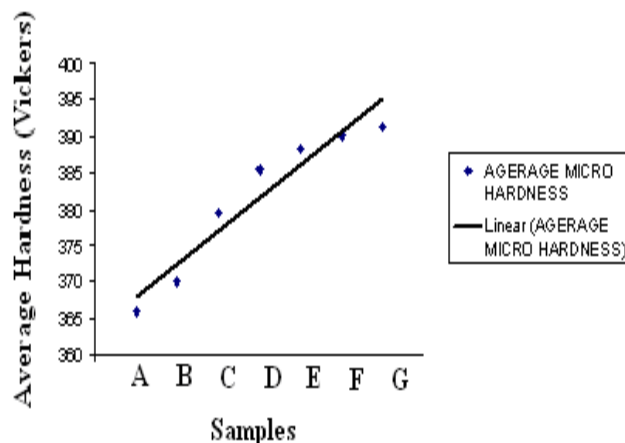


Figure 11: The plot of average microhardness value of the samples against the samples

### IV CONCLUSION

Ti6Al4V has been deposited on Ti6Al4V substrate. The laser power was varied between 0.8 - 3.0 kW while the scanning speed, powder feed rate and the gas flow rate were kept at 0.005 m/sec, 1.44 g/min and 4 l/min respectively. The effect of changing laser power on the macrostructure, microstructure and the microhardness were extensively studied. The study revealed that layer band occurred in all the samples which was characteristics of multi-layer deposition and which was attributed to be as a result of re-melting of the previous layer by the succeeding layer. Since only one layer was deposited in this study, it shows that this banding may be as result of shrinkage during solidification in the fusion zone. Also, the microstructure of the heat affected zone ranged between fine and coarse globular primary alpha as the laser power increases. A range between high and low density of columnar prior the beta grain structure were also observed. It was found that as the laser power increases, the microstructure range between fine martensite to thick martensite. The average microhardness also increases with an increase in the laser power.

### REFERENCES

- [1] Esmailian, M., Mehrvar, M., (2007). Investigation of the effect of AL<sub>2</sub>O<sub>3</sub> powder in Electro Discharge Machining for Titanium alloys, *ICME*, 9, 549-557.
- [2] Peters, M., Kumpfert, J., Ward, C.H., Leyens, C., (2003). Titanium Alloys for Aerospace Applications, in: *Titanium and Titanium Alloys, Advanced Engineering Materials*, 5, 419-427.
- [3] Cai Z., Nakajima H., Woldu M., Berglund A., Bergman M, Okabe T., (1999). In vitro corrosion resistance of titanium made using different fabrication methods. *Biomaterials*. 20(2), 183-190.
- [4] Lu, Y., Tang, H.B., Fang, Y.L., Liu, D., and Wang, H.M., (2012). Microstructure evolution of sub-critical annealed laser deposited Ti-6Al-4V alloy, *Materials and Design*, 37, 56-63.
- [5] Matthew, J. and Donachie, Jr. (1988). *TITANIUM: A Technical Guide*. Metals Park, OH: ASM International.
- [6] Wang Z.M, and Ezugwu E.O., (1997). Titanium Alloys and Their Machinability a Review. *Journal of Materials Processing Technology*, 68, 262-270.
- [7] Mazumder J and Song L. (2010). Advances in Direct Metal Deposition, A laser workshop on Laser Based Manufacturing, University of Michigan, available at <http://www.seas.virginia.edu/research/lam/pdfs/speaker%20presentations/Mazumder-NSF-IUCRC%20workshop-2010.pdf>, accessed online on 26th August 2011.
- [8] Toyserkani, E. and Khajepour, A. (2006). A mechatronics approach to laser powder deposition process. *Mechatronics*, 16(10), 631-641.

- [9] Wu, X.H., Jing, L., Mei, J.F., Mitchell, C., Goodwin, P.S. and Voice W. (2004). Microstructures of laser-deposited Ti-6Al-4V. *Materials and Design*, 25, 137-44.
- [10] Pinkerton, A. J., Wang, W. and Li, L., (2008), Component repair using laser direct metal deposition, Proc. IMechE Part B: J. Engineering Manufacture, 222, 827-836.
- [11] Mahamood, R. M., Akinlabi, E. T., Shukla M. and Pityana, S. (2012). Functionally Graded Material: An overview, *Lecture Note in Engineering*, WCE 2012, July 4-6,2012, London, United Kingdom, 3, 1593-1597.
- [12] Brandl, E., Michailov, V., Viehweger, B., Leyens, C., (2011). Deposition of Ti-6Al-4V using laser and wire, part I: Microstructural properties of single beads, *Surface & Coatings Technology*, 206, 1120-1129.
- [13] Kobryn, P. and Semiatin, S.L., (2000). Laser Forming of Ti-6Al-4V: Research Overview, in: D. Bourell, J. Beaman, R. Crawford, J. Marcus, J. Barlow (eds.), *Solid Freeform Fabrication Proceedings*, University of Texas, Austin, TX, 58-65.
- [14] Bergan, P., (2000). Implementation of laser repair processes for navy aluminum components, *Proceeding of Diminishing Manufacturing Sources and Material Shortages Conference*, (DMSMS), available at: <http://smaplab.ri.uah.edu/Smatest/Conferences/dmsms2K/papers/decamp.pdf>, accessed on 17th June 2012.
- [15] Cottam, R. and Brandt, M., (2011). Laser cladding of ti-6al-4v powder on ti-6al-4v substrate: effect of laser cladding parameters on microstructure, *Physics Procedia*, 12, 323-329.
- [16] Kobryn, P.A., and Semiatin, S.L., (2003). Microstructure and texture evolution during solidification processing of Ti-6Al-4V, *Journal of Materials Processing Technology*, vol. 135, Issues 2-3, 20 April 2003, Pages 330-339.
- [17] Messler Jr., R.W., (1999). Principles of Welding: Processes, Physics, Chemistry, and Metallurgy, WILEY-VCH, Weinheim.
- [18] Kou, S., (1987). Welding Metallurgy, John Wiley & Sons, New York.